COMPUTATIONAL ANTHROPOMORPHIC PHANTOMS FOR RADIATION PROTECTION DOSIMETRY: EVOLUTION AND PROSPECTS

CHOONSIK LEE and JAI-KI LEE[1*]
Department of Nuclear and Radiological Engineering, University of Florida, USA
[1]Department of Nuclear Engineering, Hanyang University, Korea
[*]Corresponding author. E-mail : jakilee@hanyang.ac.kr

Received February 20, 2006

Computational anthropomorphic phantoms are computer models of human anatomy used in the calculation of radiation dose distribution in the human body upon exposure to a radiation source. Depending on the manner to represent human anatomy, they are categorized into two classes: stylized and tomographic phantoms. Stylized phantoms, which have mainly been developed at the Oak Ridge National Laboratory (ORNL), describe human anatomy by using simple mathematical equations of analytical geometry. Several improved stylized phantoms such as male and female adults, pediatric series, and enhanced organ models have been developed following the first hermaphrodite adult stylized phantom, Medical Internal Radiation Dose (MIRD)-5 phantom. Although stylized phantoms have significantly contributed to dosimetry calculation, they provide only approximations of the true anatomical features of the human body and the resulting organ dose distribution. An alternative class of computational phantom, the tomographic phantom, is based upon three-dimensional imaging techniques such as magnetic resonance (MR) imaging and computed tomography (CT). The tomographic phantoms represent the human anatomy with a large number of voxels that are assigned tissue type and organ identity. To date, a total of around 30 tomographic phantoms including male and female adults, pediatric phantoms, and even a pregnant female, have been developed and utilized for realistic radiation dosimetry calculation. They are based on MRI/CT images or sectional color photos from patients, volunteers or cadavers. Several investigators have compared tomographic phantoms with stylized phantoms, and demonstrated the superiority of tomographic phantoms in terms of realistic anatomy and dosimetry calculation. This paper summarizes the history and current status of both stylized and tomographic phantoms, including Korean computational phantoms. Advantages, limitations, and future prospects are also discussed.

KEYWORDS : Radiation Dosimetry, Computational Phantom, Stylized Phantom, Tomographic Phantom

1. INTRODUCTION

Phantoms for radiation dosimetry, including physical phantoms for radiological use in medicine in particular, were introduced as early as the 1910s [1] while those for radiation protection dosimetry started to evolve in the late 1950s. This innovation was driven partly from the consensus that dose quantity for protection purposes should be assessed in "receptor conditions" instead of the traditional free-air or receptor-free conditions and partly from the availability of digital computers. Early approaches focused on the maximum dose in a body having size and composition compatible to those of the human body. The main factors considered to this end were that doses to a certain volume of interest depend on the relative position of the volume in the body as well as the penetrating power of radiation and that the specific dose distribution in the body cannot be considered in detail in radiation protection practices. Notably, there was an underlying assumption that risk to irradiated tissues or organs in the human body would not be underestimated by taking the maximum dose as the representative value.

In determination of the location and size of the maximum dose in the body, computational approaches, particularly the Monte Carlo technique, together with a computational or mathematical phantom play an invaluable role. The first version of a computational phantom was a 30 cm thick slab [2], which was followed by a right circular cylinder 30 cm in diameter and 60 cm in height [3]. In 1960, Hayes and Brucer [4] constructed compartimentalized phantoms resembling the human body. These preceded the famous Fisher and Snyder model [5] developed by some extension and refinement after the request of the Medical Internal Radiation Dose (MIRD) committee of the Society

of Nuclear Medicine for use in calculation of doses to target organs of patients from administration of nuclear pharmaceuticals. Thus, anthropomorphic phantoms were originally developed for the purpose of nuclear medicine rather than radiation protection.

In the meantime, the International Commission on Radiological Protection (ICRP) recognized the necessity of detailed assessment of doses to individual organs, because those values, even in the case of a homogeneous external radiation field, as well as the risk coefficients per unit dose, vary significantly from one organ to another. Accordingly, ICRP introduced a new dose quantity called "effective dose equivalent" for protection purposes in its 1977 recommendations [6]. The effective dose equivalent is defined as the sum of the weighted organ dose equivalent for all radio-sensitive tissues/organs in the human body and is the ultimate protection quantity representing the risk to exposed personnel. The effective dose equivalent was renamed in 1990 according to ICRP recommendations [7] as "effective dose". Since the effective dose equivalent or the effective dose is not a directly measurable quantity, use of well-defined anthropomorphic computational phantoms (hereafter abbreviated to computational phantoms) in combination with sophisticated radiation transport codes, usually Monte Carlo codes, has become a fundamental approach in modern protection dosimetry.

The computational phantoms are intended to represent the human body at a given age, having all the internal and external anatomy for which radiation risks are concerned. Remarkable progress has been made in models of computational phantoms since the early versions of MIRD phantoms were applied to radiation protection dosimetry. Two broad classes of computational phantoms exist for use in various organ dose evaluation purposes: stylized (or mathematical) phantoms and tomographic (or voxel) phantoms. This paper reviews the history of stylized and tomographic phantoms, including efforts to develop Korean computational phantoms. Advantages and disadvantages of the stylized and tomographic phantoms are analyzed and discussed, and the future prospects of computational phantoms are also discussed.

2. STYLIZED PHANTOMS

The stylized phantoms describe the shapes of the human body including internal organs by combinations of mathematical equations describing plane, cylindrical,conical, elliptical, and spherical surfaces. The revised stylized phantom was developed by Fisher and Snyder [8] at the Oak Ridge National Laboratory (ORNL) in 1966. Although the head and neck, the trunk including the arms, and the leg region were separately defined in the adult phantom, the body trunk was homogeneous without designated lung and skeleton regions, whose densities are significantly different from soft tissue. The following year, the researchers reported a revised adult phantom, where 22 internal organs and more than 100 sub-regions were defined, but the lung and skeleton were still not defined. In 1969, Snyder *et al*. [9] introduced another revised phantom composed of three different regions, the skeleton, the lungs, and soft tissue having three different material compositions. This phantom is the well-known heterogeneous stylized phantom named Medical Internal Radiation Dose (MIRD) 5 phantom.

The MIRD5 phantom is based on reference data of ICRP Publication 23 [10]. The next revised MIRD phantom was reported by the ORNL researcher group in 1978 with extensive calculation results of specific absorbed fractions [11]. Several improvements were incorporated in the revised MIRD phantom: an ellipsoidal head top, separated leg regions, male genitalia, and improved skeletal structure and gastro-intestinal tract. Kramer *et al*. [12] introduced male and female adult stylized phantoms, ADAM and EVA, which were modified from the hermaphrodite MIRD5 phantom, and they contributed to the calculation of conversion coefficients in ICRP Publication 74 [13]. Stabin *et al*. [15] developed a series of pregnant stylized phantoms for the end of each trimester of pregnancy, and utilized them to calculate internal dosimetry.

Development of adult stylized phantoms was paralleled by the construction of pediatric phantoms [4]. The early approach to develop a pediatric phantom was to uniformly scale down the adult phantom. These phantoms were known as 'similitude phantoms' since they were just small adult phantoms. However, the dimensions of body and organs of the pediatric population differ significantly from those of the adult population. Organs and organ systems differ not only in the relative amount of growth and in patterns of growth but also in their positions with respect to the body and to each other [15]. To address the problems of the similitude phantom approach, Hwang *et al*. [16,17] separately designed newborn, 1-year, and 5-year pediatric phantoms. In succession, 10-year and 15-year phantoms were developed by Jones *et al*. [18] and Deus and Poston [19], respectively.

Crysty and Eckerman [20] integrated these independent developments at the ORNL and introduced a new series of stylized phantoms of various ages in 1980. The series includes a newborn, 1-year, 5-year, 10-year, 15-year, and adult phantoms based on anthropological reference data of ICRP Publication 23 [10]. However, there was no application of the series until the next revised version was available and published in the ORNL/TM-8381 report in 1987 [21]. In this report, the 15-year phantom was assumed also to represent the adult female, and was modified according to the reference female data of ICRP 23. The report also contained a comprehensive compilation of age-dependent specific absorbed fraction calculated from the series of ORNL phantoms. The series of pediatric and adult stylized phantoms developed at the ORNL in the early 1980s has been extensively used in the evaluation of organ doses in

nuclear medicine [22,23], projection radiography [24-26], diagnostic and interventional fluoroscopy [27-29], environmental radiation exposures [30,31], and radiation protection [32-38].

Recently, several investigators have revised the largely simplified stylized organ models compared to real human anatomy. A revised head and brain model was introduced by Bouchet *et al*. and adopted by the MIRD committee for the publication of MIRD Pamphlet No. 15 [39], and a new kidney model composed of 12 interior structures was developed by the same researchers and also adopted by the MIRD committee for the publication of MIRD Pamphlet No 19 [40]. Farfan *et al*. [41] reported a new model of extrathoracic airways, trachea, and extra-pulmonary bronchi region for an adult stylized phantom. More recently, a series of revised ORNL phantoms was designed by Han *et al*. [42] wherein these new improved organ models were adopted. The phantoms are currently the most improved and revised series of stylized phantoms.

3. TOMOGRAPHIC PHANTOMS

Although stylized phantoms have significantly contributed to radiation dose evaluation and several organ models were improved, mathematical equations are inherently limited with respect to their capacity to describe complexity of the human anatomy. Demand to represent the human body more realistically was the major motivation for the development of tomographic phantoms. Concomitantly, advances in computer power and medical imaging technology have supported their evolution. Tomographic phantoms are constructed from tomographic images obtained via modern medical imaging modalities such as magnetic resonance (MR) or x-ray computed tomography (CT) of real human subjects. Some tens of organs and tissues are manually or semi-automatically segmented from the images, and the segmented two-dimensional pixel data are stacked into a three-dimensional voxel matrix where the organ features and identity are assigned to individual voxels. The resulting matrix, close to the original medical images, can more realistically describe the human anatomy than stylized phantoms.

In 1984, the first tomographic phantom, a representation of the head and trunk from CT scans of a female cadaver, was reported by Gibbs *et al*. [43-45] and the effective dose from dental radiography was calculated using the phantom. Independently, Williams *et al*. [46] also introduced tomographic phantoms in 1986 and extended this effort to construct an 8-week-old female BABY and a 7-year-old female CHILD [47,48] as well as a voxelized version of the Alderson-Rando physical phantom [49].

In 1994, Zubal *et al*. [50] segmented CT data of a diffuse melanoma patient who was scanned from head to mid-thigh to develop the Zubal Phantom. A total of 35 organs and tissues were manually segmented from 129 slices of CT images by medical staff. Afterwards, a high-resolution head phantom based on MR images of a 35-year-old male volunteer replaced the CT-based head after scaling down the original phantom. The resulting head and torso phantom was modified again by Stuchly *et al*. [51] to include the arms and legs obtained from the Visible Human date set at the US National Library of Medicine [52], and the whole body adult phantom (also called VOXTISS8) was made available in the radiation protection and medical physics community. The phantom has been freely released to the public for research purposes via a website [53], and has been widely utilized to evaluate organ dose in nuclear medicine images [54], internal radiation exposure [55-57], external radiation exposure [58,59], and radiography [60]. The phantom was modified by Kramer *et al*. [61] such that the revised phantom matched revised ICRP reference data [15]. A detailed explanation about this phantom is provided below.

Dimbylow [62] introduced NORMAN based on MRI data of a healthy volunteer in 1995. Afterwards, the voxel dimensions were scaled to match the body height and weight of the reference data of the ICRP 23[10]. Later, the NORMAN phantom was modified again to match the newer reference, the ICRP 89, with a body height of 176 cm and total body weight of 73 kg [63], and has been utilized for calibration factors calculation [64,65], magnetic field dosimetry [66,67], and internal and external radiation dosimetry [68,69]. Recently, the phantom was improved by Ferrari *et al*. [70] to include additional organs and tissues specified in the draft revision of the ICRP recommendations [71], and also applied to evaluate the effect of posture on magnetic field dosimetry [72]. In 2005, Dimbylow [73,74] introduced a female tomographic phantom, NAOMI (aNAtOMIcal model), constructed from high-resolution MRI data of a 23-year-old female subject. The phantom was rescaled to the reference height and weight of ICRP 89, and applied to the calculation of magnetic field dosimetry.

In 2000, Xu *et al*. [75] introduced the VIP-man from the sectioned color photos of Visible Human male [52]. The Visible Human data were obtained from the donated body of an executed 38-year-old male. Although the height (186 cm) and weight (90 kg) were far from the reference Caucasian data [15], the phantom currently has the highest voxel resolution, $0.33 \times 0.33 \times 1$ mm^3. Up to 1400 structures in human anatomy were manually segmented. The VIP-man has been utilized in several calculations such as internal electron dosimetry [76] and external photon, electron, neutron, and proton dosimetry [77-80]. The same research group also introduced a high-resolution tomographic head and brain phantom constructed from Visible Human male to calculate S-values for brain imaging [81], as well as a pregnant woman phantom [82,83].

Zankl *et al*. [47,48] at GSF, Germany, introduced an adult male tomographic phantom, Golem, following the precedent pediatric phantoms, BABY and CHILD, develop-

ed by researchers at the same organization. Golem was segmented from whole-body CT scan data of a 38-year-old leukemia patient. The body dimensions (176 cm in height and 68.9 kg in weight) of the patient were close to those of ICRP 89 [15]. They also constructed a visible-human from the CT data of the Visible Human male [84]. The head and torso phantom based on the CT data of a 48-year-old male subject was developed and added to the GSF voxel family. Fill *et al*. [85] have added three female tomographic phantoms of different stature, Donna, Helga, and Irene, to the GSF voxel family. A standard intestine model was constructed using a total of 300 slices of CT data obtained from a female patient in a barium enema double contrast examination, and incorporated into Donna and Irene after modification to replace the original intestines poorly segmented.

As briefly noted above, Kramer *et al*. [61] developed the MAX (Male Adult voXel) phantom by modifying the Zubal Phantom. The MAX phantom consists of the same data as the Zubal Phantom, which were obtained from three different individuals, but the arms and legs from the Visible Human (186 cm in height and 104 kg in weight) were scaled to a smaller size so that they could more accurately match the size of the Zubal Phantom body (175.3 cm in height and 70 kg in weight). Furthermore, the authors modified the organ masses of the MAX phantom to be less than 10 % matched to the ICRP 89 reference data. The MAX phantom was compared with the stylized adult male phantom, ADAM, in terms of dosimetric difference [86], and was also applied to calculate the dosimetry in a radiation accident [87]. They also introduced a female adult tomographic phantom, FAX (Female Adult voXel), segmented from 151 CT images of a 37-year-old female patient, ranging from the lower part of the head to the end of the trunk, and 206 CT images of a 62-year-old female's legs and feet [88]. The head of FAX was taken from the MAX phantom after scaling down.

Along with the development of the adult tomographic phantoms described above, there has also been growing demand to evaluate realistic age-dependent doses from internal and external radiation exposure, since the pediatric population is more susceptible to cellular DNA damage and has greater post-exposure life expectancy than adults. BABY and CHILD, introduced by Williams *et al*. [46], were the first efforts to assess the dose in the pediatric population using tomographic phantoms. Caon *et al*. [89] developed a torso tomographic phantom, ADELAIDE, from the CT data of a 14-year-old girl to calculate organ doses from CT examination. The body dimensions of the phantom were close to Australian average data for her age. Researchers at the University of Florida have taken the initiative to develop a series of pediatric tomographic phantoms following the first tomographic pediatric phantoms, UF newborn and UF 2 months, developed by Nipper *et al*. [90] from CT data of cadavers of a 6-day-old female newborn and a 2-month-old male. The organ doses from the UF newborn phantom were compared with those from the newborn ORNL phantom in pediatric radiology by Staton *et al*. [91] Recently, Lee *et al*. [92] introduced a series of head and torso pediatric tomographic phantoms, a 9-month male, a 4-year female, an 8-year female, an 11-year male, and a 14-year male, segmented from chest-abdomen-pelvis (CAP) and head CT scans. The CT data were selected from the patient CT scan database of the University of Florida Shands Children's Hospital so that normal or near-normal anatomy at their age and gender could be included. Whole body tomographic phantoms are under development by attaching arms and legs to the head and torso phantoms.

All of the tomographic phantoms described above are based on Caucasian medical images and their body dimensions are close to reference Caucasian data. Tomographic phantoms representing other ethnic groups also have been developed since the first Asian tomographic phantom, Otoko, was introduced by Saito *et al*. [93] Otoko was segmented from a whole-body CT data of a patient, whose external dimensions were in good agreement with the Japanese Reference Man [94]. Nagaoka *et al*. [95] developed male and female Japanese tomographic phantoms from high-resolution MR images of volunteers to calculate specific absorption rates of the human body exposed to an electromagnetic field. The volunteers were a 22-year-old male and female, whose body dimensions were close to the Japanese average values. The total time required for arrangement and image scanning through the whole body was approximately 8 hours for one subject.

The above comprises a short history of tomographic phantoms, the alternative approach to stylized phantoms for representing human anatomy. The features of the scanned subjects and the tomographic phantoms reported to the international community are listed in Table 1, including Korean tomographic phantoms, which are explained in the following section.

4. THE KOREAN PHANTOMS

Independent of Japanese efforts, Korean researchers have also developed non-Caucasian computational phantoms. Considerable effort has been made to establish a system of reference Korean human phantoms at Hanyang University, Korea through support from the Korean Ministry of Science and Technology. An important goal of this project was the construction of Korean computational phantoms for use in both medical and radiation protection dosimetry. First, in order to establish reference Korean organ volume data, healthy volunteers (66 males and 55 females), whose body size was close enough to the average body dimensions for Korean adults, were recruited for MR scanning. Anatomists and radiologists manually segmented internal organs and bone sites from the 121 sets of MR images, and measured the volumes of the organs and bones.

Table 1. Features of the Original Subject for Segmentation and the Resulting Tomographic Phantoms in the World

Phantom	Images	Subject	Race	Age and gender	Voxel size (mm^3)	Comment	Reference
BABY	CT	Cadaver	Caucasian	8-week-old female	2.90		[47]
CHILD	CT	Leukemia patient	Caucasian	7-year-old female	19.00		[47]
Zubal Phantom	CT	Diffuse melanoma	Caucasian	Adult male	46.70	Head and torso	[50]
NORMAN	MRI	N/A	Caucasian	Adult male	8.10		[68]
ADELAIDE	CT	Patient	Caucasian	14-year-old female	64.00	Torso	[89]
VIP-man	Photo	Cadaver	Caucasian	38-year-old male	0.10		[75]
Golem	CT	Leukemia patient	Caucasian	38-year-old male	34.60		[110]
Otoko	CT	N/A	Japanese	Adult male	9.60		[93]
UF newborn	CT	Cadaver	Caucasian	6-day-old female	0.30		[111]
UF 2 month	CT	Cadaver	Caucasian	6-month-old male	0.30		[111]
Visible-human	CT	Cadaver	Caucasian	38-year-old male	4.30	Head to knees	[84]
Frank	CT	Patient	Caucasian	48-year-old male	2.80	Head and torso	[84]
Donna	CT	Patient	Caucasian	40-year-old female	35.16		[85]
Helga	CT	Patient	Caucasian	26-year-old female	9.60	Head to mid thigh	[85]
Irene	CT	Patient	Caucasian	32-year-old female	17.58		[85]
KORMAN	MRI	Volunteer	Korean	30-year-old male	40.00		[112]
MAX	N/A	N/A	Caucasian	Adult male	46.70	Modified Zubal Phantom	[61]
FAX	CT	Volunteer	Caucasian	37-year-old female	46.70	62Y female legs	[88]
TARO	MRI	Volunteer	Japanese	22-year-old male	8.00		[95]
HANAKO	MRI	Volunteer	Japanese	22-year-old female	8.00		[95]
Pregnant woman	CT	Patient	Caucasian	30-week-pregnant female	6.20	Lower torso	[82]
NAOMI	MRI	Volunteer	Caucasian	23-year-old female	7.82		[73]
UF 9-month	CT	Patient	Caucasian	9-month-old male	0.55	Head and torso	[92]
UF 4-year	CT	Patient	Caucasian	4-year-old female	1.01	Head and torso	[92]
UF 8-year	CT	Patient	Caucasian	8-year-old female	2.02	Head and torso	[92]
UF 11-year	CT	Patient	Caucasian	11-year-old male	1.33	Head and torso	[92]
UF 14-year	CT	Patient	Caucasian	14-year-old male	2.34	Head and torso	[92]
KTMAN-1	MRI	Volunteer	Korean	25-year-old male	20.00		[100]
KTMAN-2	MRI	Volunteer	Korean	35-year-old male	20.00		[100]

The data were statistically processed, and reference volumes for 15 organs and 9 bones of Koreans were obtained [96]. Based on the reference data, two types of Korean phantoms have been developed: Korean stylized and tomographic phantoms. The development has only focused on the adult phantom thus far.

A stylized phantom of a Korean adult male was developed by Park *et al*. [97], and named KMIRD (Korean MIRD). KMIRD is based on the anthropometric and organ volume data of an average Korean adult male [96]. This is actually the second non-Caucasian stylized phantom. The first non-Caucasian stylized phantom is the Indian reference adult male phantom constructed by Biju *et al.* [98] However, the Indian phantom cannot overcome the limitations of the similitude phantom approach because only one scaling factor was uniformly applied to all equations of the outer body shape and the internal organs without matching the organ volumes to the volumes of the individual organs or to Indian reference values. As for the KMIRD, however, internal organs and body dimensions were separately scaled up or down from the original ORNL adult phantom. Mathematical models of the external body, skeleton, and a total of 13 internal organs (brain, gall bladder, heart, kidneys, liver, lungs, pancreas, spleen, stomach, testes, thymus, thyroids, and urinary bladder) were redesigned based on the ORNL adult phantom. The trunk height of the KMIRD was 8.6% smaller than that of the ORNL adult phantom. In addition, the volumes of most of the organs decreased by up to 65% (pancreas) while the brain, gall bladder wall, and thymus volumes were up to 92% (thymus) larger than those of the ORNL adult phantom. The three-dimensional frontal and rear views of the internal organs and the skeletal structure of the KMIRD are shown in Figure 1.

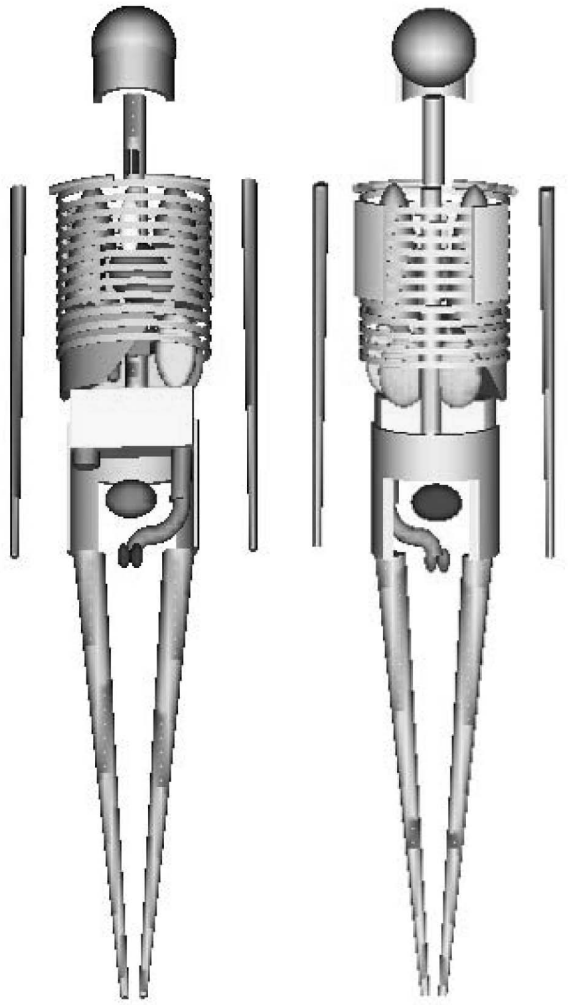

Fig. 1. The 3D Frontal (left) and Rear (right) Views of the Internal Organs and Skeletal Structure of the Korean Stylized Phantom. Skin and Muscle Were Made Transparent for Better Viewing the Internal Organs and Skeleton

Tomographic phantoms representing an average Korean adult male were developed based on MR and CT images. To acquire the source images for the phantom development, healthy adult male volunteers whose body sizes and weights were in close agreement with the average Korean adult were recruited only for the purpose of tomographic phantom development. In contrast, most existing tomographic phantoms are based upon CT images of individual patients who may or may not display average body dimensions, except for some MR-based phantoms as noted above. The first Korean tomographic male phantom, KORMAN (Korean MAN), was developed from MR images of a healthy volunteer by Lee *et al*. [99] A total of 20 internal organs and 8 bone sites were manually segmented. Since a living subject was adopted for MR scanning in the study, abdominal motion artifacts are present within the segmented digestive organs. Lower arms and hands are absent since the original MR images did not contain these parts. Skeletal structure is somewhat poorer than that of a CT image-based tomographic phantom because the skeletal tissues are not as well identified in MR images as in CT data. The resolution of the resulting phantom is $2 \times 2 \times 10$ mm^3, which is relatively poor compared with that of other CT-based tomographic phantoms. However, KORMAN contains all radio-sensitive organs required for effective dose calculation, and was a good stepping stone to develop more sophisticated Korean tomographic phantoms afterwards.

In order to resolve the relatively low resolution and motion artifacts seen in KORMAN, two approaches were employed for two different subject volunteers, whose body dimensions were also close to average Korean adult data. First, the MR image acquisition was divided into three sessions to alleviate subject fatigue resulting from long scan times. The motion of the subject was also sufficiently

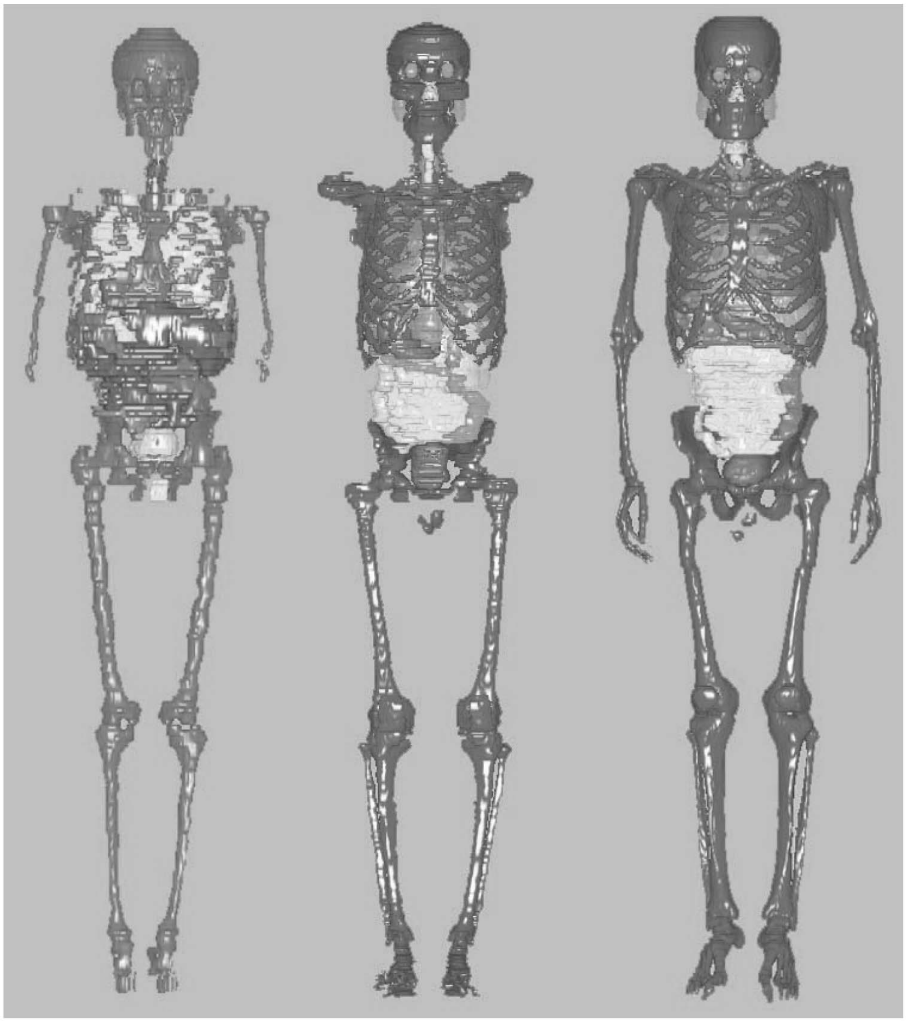

Fig. 2. Three-dimensional Views of the Korean Tomographic Phantoms, KORMAN (left), KTMAN-1 (center), and KTMAN-2 (right). Skin and Muscle Were Made Transparent for Better Viewing Internal Structure

minimized to obtain high-quality MR images. Consequently, transversal MR images of the whole body including the legs with a slice thickness of 5 mm were obtained. Second, whole-body CT images were acquired from the second volunteer using a positron emission tomography (PET)/computed tomography (CT) machine with a contrast agent, which resulted in high soft-tissue contrast. The CT modality provided much better images of the skeletal structure than previous phantoms based on MR images. The resulting MR and CT images were reviewed by experienced radiologists. A total of 29 organs and tissues, and 19 skeletal sites, were manually and semi-automatically segmented from MR and CT images: thresholding, region growing, and manual drawing referring to human atlas. The resulting phantoms, the MR-based KTMAN-1 and the CT-based KTMAN-2, have voxel array sizes of 300 × 150 × 344 voxels with a per voxel volume of 2 × 2 × 5 mm^3. Three-dimensional views of KORMAN, KTMAN-1, and KTMAN-2 are shown in Figure 2. KTMAN-1 and KTMAN-2 were recently reported by Lee *et al.* [100]

5. PROSPECTS AND CONCLUSION

Computational phantoms depicting organs and tissues of human body have been widely used in dosimetry calculation for nearly half a century. Presently, tomographic phantoms are poised to take the position of the main tool for computational dosimetry. A task group of the ICRP is at the final stage of refining the reference voxel phantoms, which incorporate the reference values of ICRP 89. This group plans to use the phantom in revision

of the dose conversion coefficients, accommodating changes in the radiation/tissue weighting factors. However, tomographic phantoms are not necessarily superior to stylized phantoms in any respect. The advantages and disadvantages of the stylized and tomographic computational anthropomorphic phantoms are as follows.

The first point is the anatomical realism described by the phantoms. Tomographic phantoms based on images of real individuals surpass stylized phantoms in terms of realism. Several investigators have revealed the unrealistic anatomy of stylized phantoms through comparison studies with tomographic phantoms for different irradiation conditions and radiation types [26,56,68,69,77,79,99,101-104]. However, anatomical limitations of tomographic phantoms also exist. The thickness of the mucosa layers in the gastrointestinal tract (less than 0.5 mm), which are radio-sensitive, cannot be described using the relatively low voxel resolution of the existing tomographic phantoms, except VIP-man whose voxel resolution is $0.33 \times 0.33 \times 1\ mm^3$ [75]. However, the stylized phantoms can precisely express the thickness of the mucosa wall [42]. Moreover, the cube-shaped voxel is reported to cause the voxel size effect, to which the surface overestimation isattributed [105,106]. On the other hand, the stylized phantoms have smooth organ surfaces free from the voxel effect.

Second, we should keep in mind that realism in modeling is related to specificity, as opposed to generality. Although the stylized phantoms are anatomically unrealistic, the volume, position, and shape of individual organs can be set so as to approximate the reference data by adjusting individual parameters of the equations. Although adjustment of voxel data in tomographic phantoms also can be done, the resulting phantoms may still reflect the original images of a particular individual, which raises questions in generality. Studies analyzing organ doses from several tomographic phantoms have reported large variability of individual organ doses even among similar size adult phantoms [100,104]. Even though the organ volume and external body dimensions are matched to reference data in order to construct the reference tomographic phantoms [61,88], the dosimetric response to internal and external radiation exposure is more dependent on the position and shape of organs rather than organ volume. In order to establish real reference tomographic phantoms, the position and shape of internal organs should be standardized in addition to organ volume.

Third, another obstacle to tomographic phantom development is that high-resolution medical images, the crucial source for phantom development, are difficult to obtain, whereas this is not in case of stylized phantoms. In spite of the long scanning time needed to obtain high-resolution MR images, motion artifacts and vague skeletal structure are inherently unavoidable in the resulting MR data. On the other hand, CT images provide high resolution and clear contrast of organ contours through the use of a contrast agent. However, significant radiation dose is transferred to the subject during whole body CT scanning and thus ethical considerations are involved.

To address these limitations of stylized and tomographic phantoms, a new approach taking advantage of features from the two kinds of phantoms has been taken by some investigators. The hybrid phantom combines the easy-to-standardize mathematical equations of stylized phantoms and the anatomical realism of tomographic phantoms. Segars *et al.* [107,108] have developed hybrid phantoms by using non-uniform rational B-splines (NURBS) technology. Xu *et al.* [109] also introduced a four-dimensional phantom converted from VIP-man by using this technology. The internal organs and body contours are segmented from medical images in the same manner used in tomographic phantom development or are converted from existing tomographic phantom data. A phantom composed of smooth NURBS surfaces is then generated from the segmented contours. Using this technology, human anatomy and smooth organ surfaces can be realistically described without any voxel effect while the organ position and shape can be easily transformed to match reference data.

Considering these advances, it is expected that computational anthropomorphic phantoms sufficiently close to real human anatomy in terms of organ position, volume and shape, as well as being matched to the reference data, will be available in the near future. These phantoms and the methodology used in their development may be very useful not only in radiation protection dosimetry but also in clinical dosimetry in nuclear medicine and radiation therapy. The latter application may be particularly promising in the future when much faster computers are available, because accurate dosimetry is crucial and patient-specific information is valuable in this application. However, we may still look back if we really need phantoms of this sophisticated for the purpose of radiation protection dosimetry. There are large variations in physical conditions among exposed individuals and, more fundamentally, there remain considerable uncertainties in the radiation weighting factors and in the risk coefficients. Under these circumstances, a remaining question is if the continued efforts to develop more realistic phantoms is beneficial enough in spite of the inevitable addition of complexity in dosimetric calculations.

REFERENCES

[1] International Commission on Radiation Units and Measurements. *Phantoms and Computational Models in Therapy, Diagnosis and Protection*, ICRU report 48, ICRU, Bethesda(1992).

[2] W.S. Snyder and J.Neufeld, "Calculated depth dose curves in tissue for broad beams of fast neutrons", *Brit. J. Radiol.* **28**(331), 342-350(1955).

[3] J.A. Auxier, W.S. Snyder and T.D. Jones, "Neutron interactions and penetration in tissue", in: *Radiation Dosimetry*, vol 1, F.H. Attix and W.C. Rosch, eds., 275-316, Academic Press, New York(1968).

[4] R.L.Hayes and M. Brucer, "Compartimentalized phantoms for the standard man, adolescent and child", *Int. J. Appl.*

Radiat. Isot., 9,113(1960).
[5] H. L. J. Fisher and W. S. Snyder, *Distribution of Dose in the Body from a Source of Gamma Rays Distributed Uniformly in an Organ*, ORNL-4168, Oak Ridge National Laboratory (1967).
[6] International Commission on Radiological Protection, *Recommendations of the ICRP, Publicatioin 26*, Pergamon Press(1977).
[7] International Commission on Radiological Protection, *1990 Recommendations of the International Commission Radiological Protection*, Publication 60, Pergamon Press(1991).
[8] H. L. J. Fisher and W. S. Snyder, *Variation of Dose Delivered by 137Cs as a Function of Body Size from Infancy to Adulthood*, ORNL-4007, Oak Ridge National Laboratory (1966).
[9] W. S. Snyder, M. R. Ford, G.G. Warner and H. L. Fisher, Jr. "MIRD Pamphlet No.5: Estimates of absorbed fractions for monoenergetic photon sources uniformly distributed in various organs of a heterogeneous phantom," *J. Nucl. Med*., **10**, 1 (1969).
[10] International Commission on Radiological Protection, "Report on the Task Group on Reference Man," ICRP Publication 23, Pergamon Press(1975).
[11] W. S. Snyder, M. R. Ford and G.G. Warner., *Revised Estimates of Absorbed Fractions for Monoenergetic Photon Sources Uniformly Distributed in Various Organs of a Heterogeneous Phantom*, MIRD Pamphlet No 5, Society of Nuclear Medicine (1978).
[12] R. Kramer, M. Zankl, G. Williams and G. Drexler, *The calculation of dose from external photon exposures using reference human phantoms and Monte-Carlo methods, Part 1: The male (ADAM) and female (EVA) adult mathematical phantoms*, GSF Bericht S-885, GSF-National Research Center for Health and Environment (1982).
[13] International Commission on Radiological Protection, *Conversion Coefficients for Use in Radiological Protection against External Radiation*, Publication 74, Pergamon Press(1996).
[14] M. G. Stabin, E. Watson and M. Cristy. *Mathematical Models and Specific Absorbed Fractions of Photon Energy in the Nonpregnant Adult Female and at the End of Each Trimester of Pregnancy*, ORNL/TM-12907, Oak Ridge National Laboratory (1995).
[15] International Commission on Radiological Protection, *Basic Anatomical and Physiological Data for Use in Radiological Protection: Reference Values*, Publication 89, Pergamon Press(2003).
[16] J. M. L. Hwang, R. L. Shoup and J. W. Poston, *Mathematical Description of a Newborn Human for Use in Dosimetry Calculations*, ORNL/TM-5453, Oak Ridge National Laboratory (1976).
[17] J. M. L. Hwang, R. L. Shoup, G. G. Warner and J.W. Poston, *Mathematical Description of a One- and Five-year-old Child for Use in Dosimetry Calculations*, ORNL/TM-5293, Oak Ridge National Laboratory (1976).
[18] R. M. Jones, J. W. Poston, J. L. M. Hwang, T.D. Jones and G.G. Warner, *The Development and Use of a Fifteen-year-old Equivalent Mathematical Phantom for Internal Dose Calculations*, ORNL/TM-5278, Oak Ridge National Laboratory (1976).
[19] S. F. Deus and J. W. Poston, "The development of a mathematical phantom representing a 10-year-old for use in internal dosimetry calculations", In *Proceedings of The Symposium on Radiopharmaceutical Dosimetry*, Oak Ridge, TN, 1976.
[20] M. Cristy, *Mathematical Phantoms Representing Children of Various Ages for Use in Estimates of Internal Dose*, ORNL/NUREG/TM-367, Oak Ridge National Laboratory (1980).
[21] M. Cristy and K. F. Eckerman, *Specific Absorbed Fractions of Energy at Various Ages from Internal Photon Sources*, ORNL/TM-8381 vol 1-7, Oak Ridge National Laboratory (1987).
[22] M. Stabin and R. Sparks, "OLINDA - PC-based software for biokinetic analysis and internal dose calculations in nuclear medicine [Abstract]," *J. Nucl. Med*., **44**, 103P (2003).
[23] M. G. Stabin, "MIRDOSE: personal computer software for internal dose assessment in nuclear medicine," *J. Nucl. Med*., **37**, 538 (1996).
[24] M. Rosenstein, *Handbook of Selected Tissue Doses for Projections Common in Diagnostic Radiology*, Food and Drug Administration (1988).
[25] D. G. Jones and B. F. Wall, *Organ Does from Medical X-ray Examinations Calculated Using Monte Carlo Techniques*, National Radiological Protection Board (1985).
[26] R. Staton, F. Pazik, J. Nipper, J. Williams, and W. Bolch. "A comparison of newborn stylized and tomographic models for dose assessment in pediatric radiology," *Phys. Med. Biol*., **48**, 805 (2003).
[27] W. Bolch, B. Pomije, J. Sessions, M. Arreola and J. Williams. "A video analysis technique for organ dose assessment in pediatric fluoroscopy: applications to voiding cystourethrograms (VCUG)," *Medical Physics*, **30**, 667 (2003).
[28] O. H. Suleiman, J. Anderson, B. Jones, G. U. Rao and M. Rosenstein, "Tissue doses in the upper gastrointestinal fluoroscopy examination," *Radiology*, **178**, 653 (1991).
[29] S. H. Stern, M. Rosenstein, L. Renaud and M. Zankl, *Handbook of Selected Tissue Doses for Fluoroscopic and Cineangiographic Examination of the Coronary Arteries*, Food and Drug Administration (1995).
[30] K. F. Eckerman and J. C. Ryman, *External Exposure to Radionuclides in Air, Water, and Soil*, U.S. Environmental Protection Agency (1993).
[31] K. Eckerman, R. Leggett, C. Nelson, J. Puskin and A. Richardson, *Cancer Risk Coefficients for Environmental Exposures to Radionuclides*, US Environmental Protection Agency (1999).
[32] International Commission on Radiological Protection, *Age-dependent Doses to Members of the Public from Intake of Radionuclides: Part 1*, Publication 56, Pergamon Press(1989).
[33] International Commission on Radiological Protection, "Age-dependent doses to members of the public from intake of radionuclides: Part 2 - ingestion dose coefficients," Publication 67, Pergamon Press(1993).
[34] International Commission on Radiological Protection, *Human Respiratory Tract Model for Radiological Protection*, Publication 66, Pergamon Press(1994).
[35] International Commission on Radiological Protection, *Age-dependent Doses to Members of the Public from Intake of Radionuclides: Part 3 - Ingestion Dose Coefficients*, Publication 69, Pergamon Press(1995).
[36] International Commission on Radiological Protection,

Age-dependent Doses to Members of the Public from Intake of Radionuclides: Part 4 - Inhalation Dose Coefficients, Publication 71, Pregamon Press(1995).

[37] International Commission on Radiological Protection, *Age-dependent Doses to Members of the Public from Intake of Radionuclides: Part 5, Compilation of Ingestion and Inhalation Dose Coefficients*, Publication 72, Pergamon Press(1996).

[38] International Commission on Radiological Protection, *Doses to the Embryo and Fetus from Intakes of Radionuclides by the Mother*, Publication 88, Pergamon Press(2001).

[39] L. G. Bouchet, W. E. Bolch, D. A. Weber, H. L. Atkins and J. W. Poston, Sr., "MIRD Pamphlet No. 15: Radionuclide S values in a revised dosimetric model of the adult head and brain. Medical Internal Radiation Dose," *J. Nucl. Med*., **40**, 62S (1999).

[40] L. Bouchet, W. Bolch, P. Blanco, B. Wessels, J. Siegel, D. Rajon, I. Clairand and G. Sgouros, "MIRD Pamphlet No. 19: Absorbed fractions and radionuclide S values for six age-dependent multi-region models of the kidney," *J. Nucl. Med*., **44**, 1113 (2003).

[41] E. Farfán, E. Han, C. Huh, T. Huston, E. Bolch and W. Bolch, "A revised stylized model of the extrathoracic and thoracic airways for use with the ICRP-66 respiratory tract model," *Health Physics*, **86**, 337 (2004).

[42] E. Y. Han, W. Bolch and K. Eckerman, "Revisions to the ORNL series of adult and pediatric computational phantoms for use with the MIRD schema," *Health Physics*, **90**,3376 (2006).

[43] S.J. Gibbs, A. Pujol, T. S. Chen and A. W. Malcolm, "Computer-Simulation of Patient Dose from Dental Radiography," *J. Dental Research*, **63**, 209 (1984).

[44] S. J. Gibbs, A. Pujol, T. S. Chen, A. W. Malcolm and A. E. James, "Patient Risk from Interproximal Radiography," *Oral Surgery Oral Medicine Oral Pathology Oral Radiology and Endodontics*, **58**, 347 (1984).

[45] S. J. Gibbs, A. Pujol, T. S. Chen, A. W. Malcolm and A. E. James, "Monte-Carlo Computation of Patient Risk from Dental Radiography," *Investigative Radiology*, **20**, S23 (1985).

[46] G. Williams, M. Zankl, W. Abmayr, R. Veit and G. Drexler, "The Calculation of Dose from External Photon Exposures Using Reference and Realistic Human Phantoms and Monte-Carlo Methods," *Phys. Med. Biol*., **31**, 449 (1986).

[47] R. Veit, M. Zankl, N. Petoussi, E. Mannweiler, G. Williams and G. Drexler, *Tomographic Anthropomorphic Models, Part I: Construction Technique and Description of Models of an 8-week-old Baby and a 7-year-old Child*, GSF-Report 3/89, GSF-National Research Center for Environment and Health (1989).

[48] M. Zankl, R. Veit, G. Williams, K. Schneider, H. Fendel, N. Petoussi and G. Drexler, "The Construction of Computer Tomographic Phantoms and Their Application in Radiology and Radiation Protection," *Radiat. Environ. Biophys*., **27**, 153 (1988).

[49] R. Veit, W. Panzer, M. Zankl and C. Scheurer, "Vergleich berechneter und gemessener Dosen an einem anthropomorphen Phantom," *Z. Med. Phys*., **2**, 123 (1992).

[50] I. G. Zubal, C. R. Harrell, E. O. Smith, Z. Rattner, G. Gindi and P. B. Hoffer, "Computerized 3-Dimensional Segmented Human Anatomy," *Medical Physics*, **21**, 299 (1994).

[51] T. W. Dawson, K. Caputa and M. A. Stuchly, "A comparison of 60 Hz uniform magnetic and electric induction in the human body," *Phys. Med. Biol*., **42**, 2319 (1997).

[52] V. M. Spitzer, D. G. Whitlock and National Library of Medicine (U.S.), *Atlas of the Visible Human Male : Reverse Engineering of the Human Body*, Jones and Bartlett, Sudbury, Mass. (1998).

[53] I. G. Zubal, The Zubal Phantom:http://noodle.med.yale.edu/zubal/.

[54] I. G. Zubal and C. R. Harrell, "Voxel-Based Monte-Carlo Calculations of Nuclear-Medicine Images and Applied Variance Reduction Techniques," *Image and Vision Computing*, **10**, 342 (1992).

[55] M. G. Stabin and H. Yoriyaz, "Photon specific absorbed fractions calculated in the trunk of an adult male voxel-based phantom," *Health Physics*, **82**, 21 (2002).

[56] H. Yoriyaz, A. dos Santos, M. G. Stabin and R. Cabezas, "Absorbed fractions in a voxel-based phantom calculated with the MCNP-4B code," *Medical Physics*, **27**, 1555 (2000).

[57] H. Yoriyaz, M. G. Stabin and A. dos Santos, "Monte Carlo MCNP-4B-based absorbed dose distribution estimates for patient-specific dosimetry," *J. Nucl. Med*., **42**, 662 (2001).

[58] S. Chiavassa, M. Bardies, F. Guiraud-Vitaux, D. Bruel, J. R. Jourdain, D. Franck and I. Aubineau-Laniece, "OEDIPE: A personalized dosimetric tool associating voxel-based models with MCNPX," *Cancer Biotherapy and Radiopharmaceuticals*, **20**, 325 (2005).

[59] S. Chiavassa, A. Lemosquet, I. Aubineau-Laniece, L. de Carlan, I. Clairand, L. Ferrer, M. Bardies, D. Franck and M. Zankl, "Dosimetric comparison of Monte Carlo codes (EGS4, MCNP, MCNPX) considering external and internal exposures of the Zubal phantom to electron and photon sources," *Radiation Protection Dosimetry*, **116**, 631 (2005).

[60] D. R. Dance, G. H. McVey, M. Sandborg, G. A. Carlsson and F. R. Verdun, "The optimisation of lumbar spine AP radiography using a realistic computer model," *Radiation Protection Dosimetry*, **90**, 207 (2000).

[61] R. Kramer, J. W. Vieira, H. J. Khoury, F. R. A. Lima and D. Fuelle, "All about MAX: a male adult voxel phantom for Monte Carlo calculations in radiation protection dosimetry," *Phys. Med.Biol*., **48**, 1239 (2003).

[62] P. J. Dimbylow, "The development of realistic voxel phantoms for electromagnetic field dosimetry," In *Proceedings of Int. Workshop on Voxel Phantom Development*, Chilton, UK, 1995.

[63] P. J. Dimbylow, "FDTD calculations of the whole-body averaged SAR in an anatomically realistic voxel model of the human body from 1 MHz to 1 GHz," *Phys.Med.Biol*., **42**, 479 (1997).

[64] J. G. Hunt, I. Malatova and S. Foltanova, "Calculation and measurement of calibration factors for bone surface seeking low energy gamma emitters and determination of Am-241 activity in a real case of internal contamination," *Radiation Protection Dosimetry*, **82**, 215 (1999).

[65] J. G. Hunt, I. Malatova, S. Foltanova and B. M. Dantas, "Calibration of in vivo measurement systems using a voxel phantom and the Monte Carlo technique," *Radiation Protection Dosimetry*, **89**, 283 (2000).

[66] P. J. Dimbylow, "Induced current densities from low-frequency magnetic fields in a 2 mm resolution, anatomically realistic model of the body," *Phys. Med. Biol*., **43**, 221 (1998).

[67] P. J. Dimbylow, "Fine resolution calculations of SAR in

the human body for frequencies up to 3 GHz," *Phys. Med. Biol.*, **47**, 2835 (2002).
[68] D. G. Jones, "A realistic anthropomorphic phantom for calculating organ doses arising from external photon irradiation," *Radiation Protection Dosimetry*, **72**, 21 (1997).
[69] D. G. Jones, "A realistic anthropomorphic phantom for calculating specific absorbed fractions of energy deposited from internal gamma emitters," *Radiation Protection Dosimetry*, **79**, 411 (1998).
[70] P. Ferrari and G. Gualdrini, "An improved MCNP version of the NORMAN voxel phantom for dosimetry studies," *Phys. Med. Biol.*, **50**, 4299 (2005).
[71] International Commission on Radiological Protection, *Recommendation of the International Commission on Radiological Protection*, ICRP DRAFT 2005(2005).
[72] R. P. Findlay and P. J. Dimbylow, "Effects of posture on FDTD calculations of specific absorption rate in a voxel model of the human body," *Phys. Med. Biol.*, **50**, 3825 (2005).
[73] P. Dimbylow, "Development of the female voxel phantom, NAOMI, and its application to calculations of induced current densities and electric fields from applied low frequency magnetic and electric fields," *Phys. Med. Biol.*, **50**, 1047 (2005).
[74] P. Dimbylow, "Resonance behaviour of whole-body averaged specific energy absorption rate (SAR) in the female voxel model, NAOMI," Phys. Med. Biol., 50, 4053 (2005).
[75] X. G. Xu, T. C. Chao and A. Bozkurt, "VIP-man: An image-based whole-body adult male model constructed from color photographs of the visible human project for multi-particle Monte Carlo calculations," *Health Physics*, **78**, 476 (2000).
[76] T. C. Chao and X. G. Xu, "Specific absorbed fractions from the image-based VIP-Man body model and EGS4-VLSI Monte Carlo code: internal electron emitters," *Phys. Med. Biol.*, **46**, 901 (2001).
[77] A. Bozkurt, T. C. Chao and X. G. Xu, "Fluence-to-dose conversion coefficients from monoenergetic neutrons below 20 MeV based on the VIP-Man anatomical model," *Phys. Med. Biol.*, **45**, 3059 (2000).
[78] A. Bozkurt, T. C. Chao and X. G. Xu, "Fluence-to-dose conversion coefficients based on the VIP-MAN anatomical model and MCNPX code for monoenergetic neutrons above 20 MeV," *Health Physics*, **81**, 184 (2001).
[79] A. Bozkurt and X. G. Xu, "Fluence-to-dose conversion coefficients for monoenergetic proton beams based on the VIP-Man anatomical model," *Radiation Protection Dosimetry*, **112**, 219 (2004).
[80] T. C. Chao, A. Bozkurt and X. G. Xu, "Organ dose conversion coefficients for 0.1-10 MeV electrons calculated for the VIP-MAN tomographic model," *Health Physics*, **81**, 203 (2001).
[81] T. C. Chao and X. G. Xu, "S-values calculated from a tomographic head/brain model for brain imaging," *Physics in Medicine and Biology*, **49**, 4971 (2004).
[82] C. Y. Shi and X. G. Xu, "Development of a 30-week-pregnant female tomographic model from computed tomography (CT) images for Monte Carlo organ dose calculations," *Medical Physics*, **31**, 2491 (2004).
[83] C. Y. Shi, X. G. Xu and M. G. Stabin, "Specific absorbed fractions for internal photon emitters calculated for a tomographic model of a pregnant woman," *Health Physics*, **87**, 507 (2004).
[84] N. Petoussi-Henss, M. Zankl, U. Fill and D. Regulla, "The GSF family of voxel phantoms," *Phys. Med. Biol.*, **47**, 89 (2002).
[85] U. A. Fill, M. Zankl, N. Petoussi-Henss, M. Siebert and D. Regulla, "Adult female voxel models of different stature and photon conversion coefficients for radiation protection," *Health Physics*, **86**, 253 (2004).
[86] R. Kramer, J. W. Vieira, H. J. Khoury and F. D. Lima, "MAX meets ADAM: a dosimetric comparison between a voxel-based and a mathematical model for external exposure to photons," *Phys. Med. Biol.*, **49**, 887 (2004).
[87] R. Kramer, A. M. Santos, C. A. O. Brayner, H. J. Khoury, J. W. Vieira and F. R. A. Lima, "Application of the MAX/EGS4 exposure model to the dosimetry of the Yanango radiation accident," *Phys. Med. Biol.*, **50**, 3681 (2005).
[88] R. Kramer, H. J. Khoury, J. W. Vieira, E. C. M. Loureiro, V. J. M. Lima, F. R. A. Lima and G. Hoff, "All about FAX: a female adult voxel phantom for Monte Carlo calculation in radiation protection dosimetry," *Phys. Med. Biol.*, **49**, 5203 (2004).
[89] M. Caon, G. Bibbo, and J. Pattison, "An EGS4-ready tomographic computational model of a 14-year-old female torso for calculating organ doses from CT examinations," Phys. *Med. Biol.*, **44**, 2213 (1999).
[90] J. Nipper, J. Williams, and W. Bolch, "Creation of two tomographic voxel models of pediatric patients in the first year of life," *Phys. Med. Biol.*, **47**, 3143 (2002).
[91] R. J. Staton, F. D. Pazik, J. C. Nipper, J. L. Williams and W. E. Bolch, "A comparison of newborn stylized and tomographic models for dose assessment in pediatric radiology," *Phys. Med.Biol.*, **48**, 805 (2003).
[92] C. Lee, J. Williams, C. Lee and W. Bolch, "The UF series of tomographic computational phantoms of pediatric patients," *Medical Physics*, **32**, 3537 (2005).
[93] K. Saito, A. Wittmann, S. Koga, Y. Ida, T. Kamei, J. Funabiki and M. Zankl, "Construction of a computed tomographic phantom for a Japanese male adult and dose calculation system," *Radiat. Environ. Biophys.*, **40**, 69 (2001).
[94] G. Tanaka, Y. Nakahara, and Y. Nakazima, "Japanese reference man 1988-IV. Studies on the weight and size of internal organs of Normal Japanese," *Nippon Igaku Hoshasen Gakkai Zasshi*, **49**, 344 (1989).
[95] T. Nagaoka, S. Watanabe, K. Sakurai, E. Kunieda, S. Watanabe, M. Taki and Y. Yamanaka, "Development of realistic high-resolution whole-body voxel models of Japanese adult males and females of average height and weight, and application of models to radio-frequency electromagnetic-field dosimetry," *Phys. Med.Biol.*, **49**, 1 (2004).
[96] S. Park, J. Lee, J. I. Kim, Y. J. Lee, Y. K. Lim, C. S. Kim and C. Lee, "In vivo organ mass of Korean adults obtained from whole body magnetic resonance data," *Radiation Protection Dosimetry*, (in press).
[97] S. Park, C. Lee and J. Lee, "Construction of MIRD-type Korean reference adult male and female phantoms.," *Health Physics*, **84**, S164 (2003).
[98] K. Biju and P. S. Nagarajan, "Computed normalized

effective doses to an Indian adult in conventional diagnostic X ray chest examinations," *Radiation Protection Dosimetry*, **88**, 119 (2000).
[99] C. Lee, J. Lee and C. Lee, "Korean adult male voxel model KORMAN segmented from magnetic resonance images," *Medical Physics*, **31**, 1017 (2004).
[100] C. Lee, C. Lee, S. Park and J. Lee, "Development of the two Korean adult tomographic computational phantoms for organ dosimetry," *Medical Physics*, **33**, 380 (2006).
[101] T. C. Chao, A. Bozkurt and X. G. Xu, "Conversion coefficients based on the VIP-MAN anatomical model and EGS4-VLSI code for external monoenergetic photons from 10 keV to 10 MeV," *Health Physics*, **81**, 163 (2001).
[102] R. Kramer, H. J. Khoury and J. W. Vieira, "Comparison between effective doses for voxel-based and stylized exposure models from photon and electron irradiation," *Phys. Med. Biol*., **50**, 5105 (2005).
[103] C. Lee and J. Lee, "The dosimetric effect of unrealistic arm structure of stylized human model," *Medical Physics*, **32**, 2100 (2005).
[104] M. Zankl, U. Fill, N. Petoussi-Henss and D. Regulla., "Organ dose conversion coefficients for external photon irradiation of male and female voxel models," *Phys. Med. Biol*., **47**, 2367 (2002).
[105] D. A. Rajon, D. W. Jokisch, P. W. Patton, A. P. Shah, C. J. Watchman and W. E. Bolch, "Voxel effects within digital images of trabecular bone and their consequences on chord-length distribution measurements," *Phys. Med. Biol*., **47**, 1741 (2002).
[106] D. A. Rajon, P. W. Patton, A. P. Shah, C. J. Watchman and W. E. Bolch, "Surface area overestimation within three-dimensional digital images and its consequence for skeletal dosimetry," *Medical Physics*, **29**, 682 (2002).
[107] W. P. Segars, D. S. Lalush and B. M. W. Tsui, "A realistic spline-based dynamic heart phantom," *IEEE Transactions on Nuclear Science*, **46**, 503 (1999).
[108] W. P. Segars, B. M. W. Tsui, E. C. Frey, G. A. Johnson and S. S. Berr, "Development of a 4-D digital mouse phantom for molecular imaging research," *Molecular Imaging and Biology*, **6**, 149 (2004).
[109] G. Xu and C. Shi, "Preliminary development of a 4D anatomical model for Monte Carlo simulation," *In Proceedings of The Monte Carlo Method: Versatility Unbounded in a Dynamic Computing World*, Chattanooga, TN, 2005.
[110] M. Zankl, and A. Wittmann, "The adult male voxel model "Golem" segmented from whole-body CT patient data," *Radiat. Environ. Biophys*., **40**, 153 (2001).
[111] J. C. Nipper, J. L. Williams and W. E. Bolch, "Creation of two tomographic voxel models of pediatric patients in the first year of life," *Phys. Med. Biol*., **47**, 3143 (2002).
[112] C. Lee, C. Lee and J. Lee, "Korean adult male voxel model KORMAN segmented from magnetic resonance images," *Medical Physics*, **31**, 1017 (2004).